Galaxy Evolution and Feedback across Different Environments
Proceedings IAU Symposium No. 359, 2020
T. Storchi-Bergmann, W. Forman, R. Overzier & R. Riffel, eds.
doi:10.1017/S1743921320002446

Nuclear ionised outflows in a sample of 30 local galaxies

D. Ruschel-Dutra[1], T. Storchi-Bergmann[2] and A. Schnorr-Müller[2]

[1]Departamento de Física, Universidade Federal de Santa Catarina, P.O. Box 476, 88040-900, Florianópolis, SC, Brazil
e-mail:daniel.ruschel@ufsc.br

[2]Instituto de Física, Universidade Federal do Rio Grande do Sul, Av. Bento Goncalves 9500, 91501-970 Porto Alegre, RS, Brazil

Abstract. Understanding active galactic nuclei (AGN) feedback is essential for building a coherent picture of the evolution of the super massive black hole and its host galaxy. To that end we have analysed the inner kiloparsec of a sample of 30 local AGN with spatially resolved optical spectroscopy. In this talk I will review the analysis of the ionised gas for the galaxies in our sample, including kinematical maps, emission line ratios and fluxes. The W_{80} kinematical index is used to trace outflows, and also to provide an estimate for the outflowing velocity. Electron densities, derived from the [S II] $\lambda\lambda$6716, 6731Å lines, along with Hα luminosities and the sizes of the outflowing regions are employed in estimates of the outflowing gas mass. We find a median mass outflow rate of $\dot{M} = 0.3$ M$_\odot$ yr^{-1} and median outflow power of $\log[P/(\mathrm{erg\,s^{-1}})] = 40.4$.

Keywords. active galactic nuclei, feedback, ionised gas

1. Introduction

The discovery of correlations between the mass of the central supermassive black hole (SMBH) and properties of the host galaxy, such as the host spheroid mass and velocity dispersion (Ferrarese & Merritt 2000; Gültekin *et al.* 2009; Kormendy & Ho 2013; van den Bosch 2016), and the similar evolution of the cosmic star formation rate (SFR) density and the black hole accretion rate density (Madau & Dickinson 2014) points to the growth of the SMBH being closely linked to the assembly of stellar mass of the host galaxy. It is believed that this link emerges due to both the mass transfer to the inner region of the galaxy that also feeds the SMBH (Storchi-Bergmann & Schnorr-Müller 2019) and the regulating effect of feedback from the triggered active galactic nuclei (AGN) on the star formation in the host galaxy. The effect of AGN feedback is supported by cosmological simulations and models of galaxy evolution (Springel *et al.* 2005; Vogelsberger *et al.* 2014; Schaye *et al.* 2015), as they require such feedback to reproduce observables such as the shape of the galaxy luminosity function, the colour bimodality of the galaxy population in the local universe, and the low star formation efficiency in the most massive galaxies (Alexander & Hickox 2012; Fabian 2012; Harrison 2017).

The main goal here is to probe the gas excitation and kinematics within the inner kiloparsec of the host galaxies at spatial resolution down to a few tens of parsecs in order to resolve the relevant processes of feeding and feedback of the AGN at the nucleus. In this contribution, mass-outflow rates and outflow kinetic power are based on the W_{80} index, defined as the width in velocity space that encompasses 80 per cent of the emission line

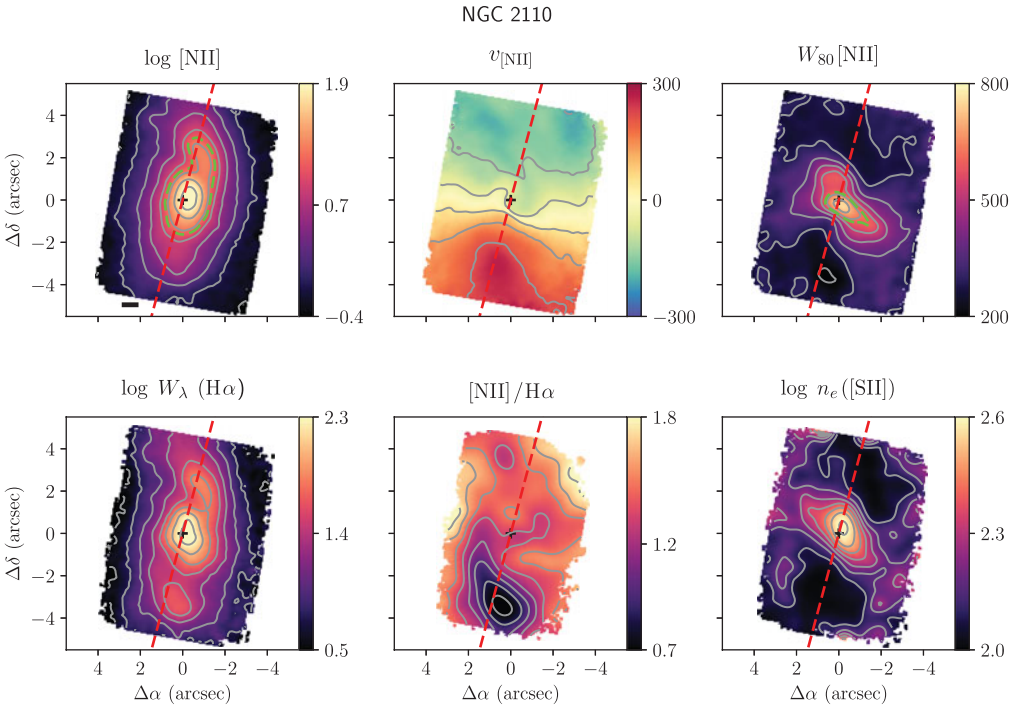

Figure 1. Example of quantities derived from the emission line fitting for NGC 2110. From left to right and top to bottom the panels show: i) the logarithm of the flux in units of 10^{-15} erg s^{-1} cm^{-2} arcsec^{-2}; ii) the radial velocity in units of km s^{-1}; iii) the W_{80} index also in units of km s^{-1}; iv) the logarithm of the equivalent width of the Hα line in Å; v) the flux ratio between the [N II] and the Hα lines; vi) and the electron density derived from the [S II] lines. The green contour in the W_{80} panel highlights the region where $W_{80} \geqslant 600$ km s^{-1}, and thus spectra within this contour are classified as outflow dominated.

flux. We also compare our results with those of previous studies relating these quantities to the AGN luminosity (e.g. Fiore *et al.* 2017).

2. Data

Our sample comprises 30 AGN observed with the Gemini instruments GMOS-IFUs (North and South), up until the observing semester 2017A, and limited to a redshift of $z \leqslant 0.03$. Out of the 30 galaxies in the sample, 17 have a counterpart in the 70 month Swift/BAT (hereafter SB70) catalogue (Baumgartner et al. 2013). The remaining 7 less luminous sources are either LINERS or Sy2's, including at least one known galaxy (NGC 4180) harbouring a Compton-thick AGN.

The data used in this study comes from many observing runs, although with similar setups, obtained with the Gemini Multi-Object Spectrographs (GMOS) integral field units (IFUs) (Allington-Smith et al. 2002) both at the northern and southern Gemini telescopes. The gratings used in these observations, namely B600 and R400, have a resolving power of $R \sim 1800$, which translates to emission-line widths FWHM of ∼50 km/s. [O III]and Hβ lines are available for 19 galaxies of the sample observed in single slit mode, covering the wavelength range ≈ 4800–7000Å, while the other 11 targets have spectra in the range ≈5600–7000Å. Angular resolutions vary between 0.6 and 1.0 arcsec, depending on the seeing. Fig. 1 shows an example of the quantities derived from the emission line fitting of the data cubes.

https://doi.org/10.1017/S1743921320002446 Published online by Cambridge University Press

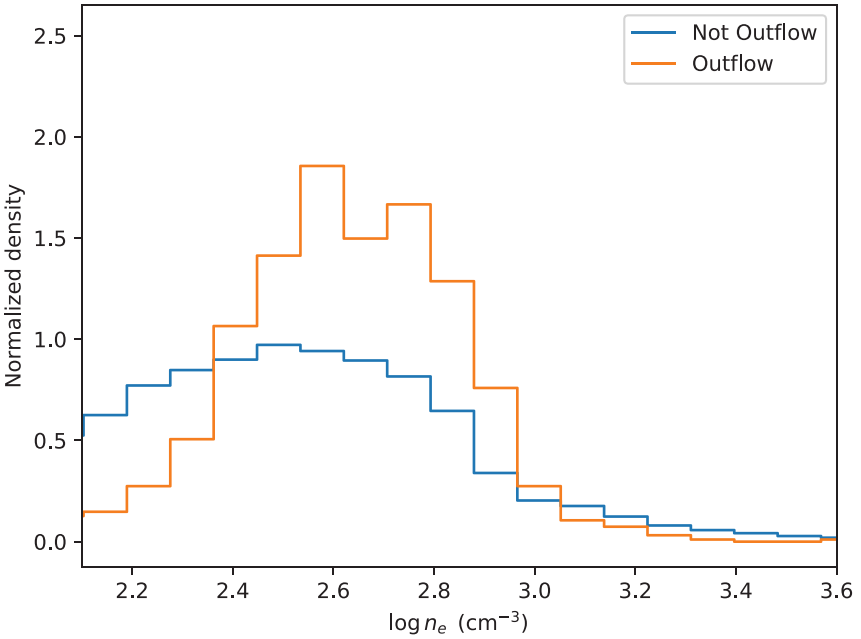

Figure 2. Histogram of electron densities measured in spaxels identified as outflow dominated (*orange*), and not outflow dominated (*blue*), in units of cm^{-3}. Spectra for which the NLR has an outflow component are usually denser and have a narrower range of densities.

3. Results and Discussion

In order to quantify the outflows, we identified the spaxels in which the ionised gas kinematics is not compatible with disk rotation. A spaxel is defined as being part of an outflow, or having its nebular emission dominated by outflowing gas, based on the following criteria: i) $W_\lambda(H\alpha) > 6$Å to ensure an accurate value for $L_{\mathrm{H}\alpha}$; ii) the velocity dispersion, measured by W_{80} of the [N II] λ6583Å or [O III] 5007Å line, must be above 600 km s^{-1}, a limit which excludes reasonable expectations for bound orbits even in the most massive galaxies; iii) it has at least four contiguous neighbouring spaxels also matching the first two criteria, which warrants against spurious detection, since the FWHM of the point spread function is at best 3 spaxels. Out of 28 galaxies with well constrained emission line fits, 12 are classified as having outflows if we apply the above mentioned criteria to the [N II] λ6583Å line. The two excluded galaxies are NGC 1068 and Mrk 6 which have some caveats that are beyond the scope of this communication.

Using the [S II] lines $\lambda\lambda$6716, 6731Å we have estimated the electron densities for all the spaxels in the sample, adopting a fixed standard electron temperature of 10^4 K, and applying the relation described in Proxauf *et al.* (2014). Figure 2 shows the histogram of electron densities for spectra identified as outflows and for those we do not classify as outflows. The histogram is given in units of probability density, which means that the integral of the histogram equals unity. Median values are 257^{+351}_{-157} cm^{-3} and 414^{+282}_{-170} cm^{-3} for the non-outflow and outflow samples respectively, where the upper and lower limits are the distances from the median to the 16% and 84% percentiles. Our main conclusion in this regard is that there is a clear tendency towards higher density for regions where the ionised gas emission is characteristic of outflows. This could be interpreted as the result of shocks between the outflowing gas and the interstellar medium. However, it is also possible that in some cases the high values of W_{80} are caused by two gas systems which are superimposed on our line of sight, and not necessarily interacting.

https://doi.org/10.1017/S1743921320002446 Published online by Cambridge University Press

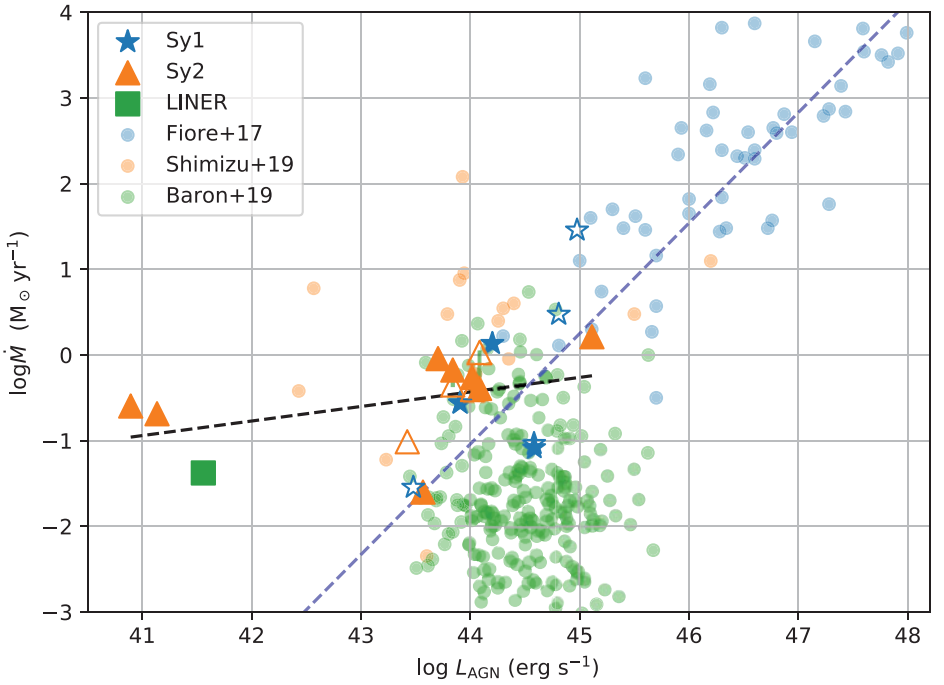

Figure 3. Relation between AGN bolometric luminosities and mass outflow rates based on [O III](*open symbols*) and [N II] (*filled symbols*) emission. The blue line represents the best fit from Fiore *et al.* (2017), and the circles are points from Fiore *et al.* (2017) (*blue*), Shimizu *et al.* (2019) (*orange*) and Baron & Netzer (2019) (*green*).

We begin our discussion of mass outflow rates by first considering the ionised gas mass, which was evaluated for each individual spaxel of each galaxy as given by

$$M = \frac{m_p L_{\mathrm{H}\alpha}}{n_e j_{\mathrm{H}\alpha}(T)} \tag{3.1}$$

where m_p is the proton mass, n_e is the number density of electrons from the [S II] lines flux ratio, $L_{\mathrm{H}\alpha}$ is the Hα luminosity and $j_{\mathrm{H}\alpha}$ is the Hα emissivity in erg cm^3 s^{-1} for a given temperature. Since we did not measure the temperature based on the nebular emission, we assume a standard value of 10^4 K. Mass outflow rates are given by equation 3.2, which follows from the basic assumption that the outflow velocity $v = W_{80}/2$, is approximately the average velocity of the gas since it left the vicinity of the AGN. Therefore, the time it took for the gas to reach its current distance from the central engine is R/v.

$$\dot{M} = M\frac{v}{R} \tag{3.2}$$

The distance R is assumed to be the distance, projected onto the plane of the sky, of the farthest spectrum classified as being outflow dominated. Underlying this assumption is a model which considers the outflow to be spherically symmetrical. This rather crude simplification ignores any differences in the geometry of the outflows, however it does allow for a homogenous treatment of the sample.

Our main results are shown in figures 3 and 4, which show the relation between mass outflow rates and outflow kinetic power to the bolometric luminosity of the AGN. Most of the galaxies in our sample, which were identified as having outflows, lie in the same region of the estimates from previous works on the subject (Fiore *et al.* 2017; Baron & Netzer 2019; Shimizu *et al.* 2019). However, we find that three objects with luminosities

https://doi.org/10.1017/S1743921320002446 Published online by Cambridge University Press

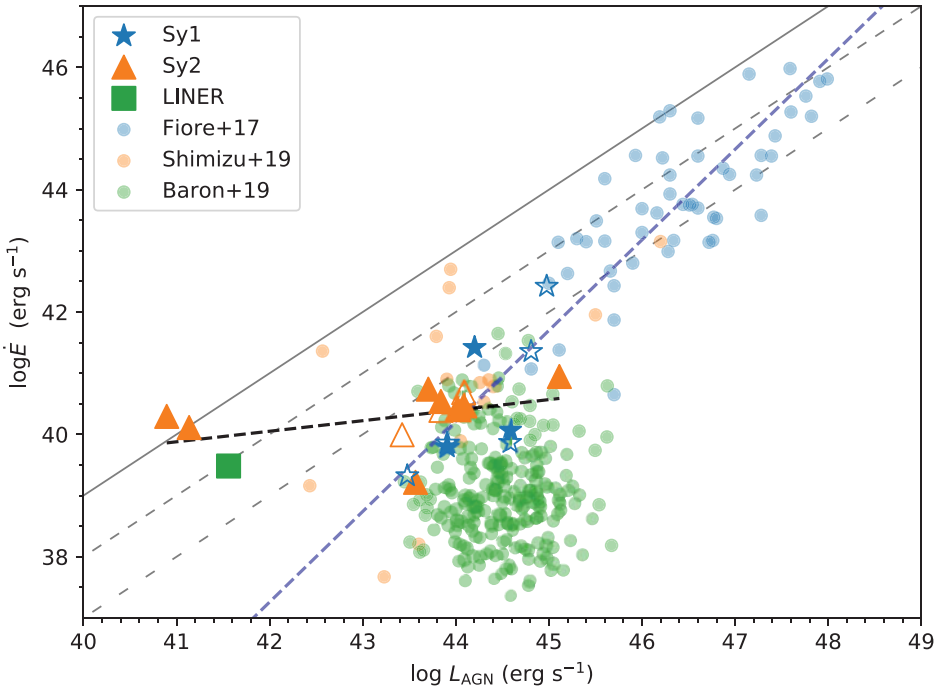

Figure 4. Outflow kinetic power vs. AGN bolometric luminosity. Solid and dashed black lines represent the ratios 1/10, 1/100 and 1/1000. The symbols are the same as in Fig. 3.

below 10^{42} erg s^{-1} show mass outflow rates that are unexpectedly high. We we look at the kinetic power carried out by these outflows (Fig. 4), we see that they are between having 1 and 10 per cent of the bolometric luminosity of the AGN. In the present study, estimates based on [O III] and [N II] emission yield similar results, for both mass outflow rates and outflow kinetic power, however, since only half of our sample has spectral coverage which includes the λ5007Å [O III] line, we will focus on the more representative [N II] emission. Based on the 12 galaxies for which the [N II] emission shows signs of outflowing gas, we find a median mass outflow rate of $\dot{M} = 0.3$ M$_\odot$ yr^{-1}, and a median outflow power of $\log P = 40.4$ erg s^{-1}. Considering the bolometric luminosities we see that, for the majority of the sources considered, the energy carried out in the form of outflows is less than one per cent of the total energy irradiated by the AGN.

References

Alexander, D. M. & Hickox, R. C. 2012, *New A Rev.*, 56, 93
Allington-Smith, J., *et al.* 2002, *PASA*, 114, 892
Baron, D. & Netzer, H. 2019, *MNRAS*, 482, 3915
Baumgartner, W. H., Tueller, J., Markwardt, C. B., *et al.* 2013, *ApJS series*, 207, 19
Fabian, A. 2012, *ARA&A*, 50, 455
Ferrarese, L. & Merritt, D. 2000, *ApJ*, 539, L9
Fiore, F., *et al.* 2017, *A&A*, 601, A143
Gültekin, K., *et al.* 2009, *ApJ*, 698, 198
Harrison, C. M. 2017, *Nature Astronomy*, 1, 0165
Kormendy, J. & Ho, L. C. 2013, *ARA&A*, 51, 511
Madau, P. & Dickinson, M. 2014, *ARA&A*, 52, 415
Proxauf, B., Öttl, S., & Kimeswenger, S. 2014, *A&A*, 561, A10
Schaye, J., *et al.* 2015, *MNRAS*, 446, 521

https://doi.org/10.1017/S1743921320002446 Published online by Cambridge University Press

Shimizu, T. T., *et al.* 2019, *MNRAS*, 490, 5860
Springel, V., Di Matteo, T., & Hernquist, L. 2005, *MNRAS*, 361, 776
Storchi-Bergmann, T. & Schnorr-Müller, A. 2019, *Nature Astronomy*, 3, 48
Vogelsberger, M., *et al.* 2014, *Nature*, 509, 177
van den Bosch, R. C. E., 2016, *ApJ*, 831, 134

https://doi.org/10.1017/S1743921320002446 Published online by Cambridge University Press